

## Article

# Exploring the Potential of Sentinel-1 Ocean Wind Field Product for Near-Surface Offshore Wind Assessment in the Norwegian Arctic

Eduard Khachatryan <sup>1,\*</sup>, Patricia Asemann <sup>1,\*</sup>, Lihong Zhou <sup>1</sup>, Yngve Birkelund <sup>1</sup>, Igor Esau <sup>1,2</sup> and Benjamin Ricaud <sup>1</sup>

<sup>1</sup> Department of Physics and Technology, UiT The Arctic University of Norway, NO-9037 Tromsø, Norway

<sup>2</sup> Nansen Environmental and Remote Sensing Center, NO-5007 Bergen, Norway

\* Correspondence: eduard.khachatryan@uit.no (E.K.); patricia.asemann@uit.no (P.A.)

† These authors contributed equally to this work.

**Abstract:** The exploitation of offshore wind resources is a crucial step towards a clean energy future. It requires an advanced approach for high-resolution wind resource evaluations. We explored the suitability of the Sentinel-1 Level-2 OCN ocean wind field (OWI) product for offshore wind resource assessments. The SAR data were compared to in situ observations and three reanalysis products: the global reanalysis ERA5 and two regional reanalyses CARRA and NORA3. This case study matches 238 scenes from 2022 for the Goliat station, an oil platform located 85 km northwest of Hammerfest in the Barents Sea, where a new offshore wind park has been proposed. The analysis showed that despite their unique limitations in spatial and temporal resolutions, all data sources have similar statistical properties (RMSE, correlation coefficient, and standard deviation). The Weibull parameters characterizing the wind speed distributions showed strong similarities between the Sentinel-1 and all reanalysis data. The Weibull parameters of the in situ measurements showed an underestimation of wind speed compared to all other sources. Comparing the full reanalysis datasets with the subsets matching the SAR scenes, only slight changes in Weibull parameters were found, indicating that, despite its low temporal resolution, the Sentinel-1 Level 2 OWI product can compete with the more commonly used reanalysis products in the estimation of offshore wind resources. Its high spatial resolution, which is unmatched by other methods, renders it especially valuable in offshore areas close to complex coastlines and in resolving weather events at a smaller scale.

**Keywords:** offshore wind; renewable energy; synthetic aperture radar; reanalysis data; Sentinel-1; Arctic



**Citation:** Khachatryan, E.; Asemann, P.; Zhou, L.; Birkelund, Y.; Esau, I.; Ricaud, B. Exploring the Potential of Sentinel-1 Ocean Wind Field Product for Near-Surface Offshore Wind Assessment in the Norwegian Arctic. *Atmosphere* **2024**, *15*, 146. <https://doi.org/10.3390/atmos15020146>

Academic Editor: William Cheng

Received: 26 December 2023

Revised: 17 January 2024

Accepted: 22 January 2024

Published: 24 January 2024



**Copyright:** © 2024 by the authors. Licensee MDPI, Basel, Switzerland. This article is an open access article distributed under the terms and conditions of the Creative Commons Attribution (CC BY) license (<https://creativecommons.org/licenses/by/4.0/>).

## 1. Introduction

The rapid exploitation of renewable and sustainable energy sources plays a pivotal role in the resolution of the current global environmental crisis. In this context, offshore wind power production has emerged as one of the most promising technologies available. According to the International Energy Agency, offshore wind has the potential to cover the current global energy demand many times over [1]. Innovations in turbine capacities, foundations, and energy transmission continue to promote this technology and drive down the costs of offshore wind energy production. Despite its high regional advantage, Norway's offshore wind resources remain largely untapped [1].

The first step towards the realization of new offshore wind power plants is the selection of high-quality locations, that is, those with high mean wind speed and minimal wind variability while being relatively close to the shore. Preliminary wind resource assessments are particularly difficult in offshore regions due to the sparseness of in situ observations. Reanalysis products offer a more consistent and long-term coverage. However, they also entail a number of drawbacks such as low spatial resolution, poor performance in coastal

areas, and a general underestimation of wind speed compared to in situ measurements [2,3]. Remote sensing data from synthetic aperture radar (SAR) offers a complementary source of information on near-surface offshore wind.

In light of the ambitious goals of the Norwegian government in terms of developing offshore wind, a comprehensive evaluation and intercomparison of all sources of wind data available for the Norwegian offshore region is crucial. Most offshore wind energy projects commissioned today are placed within 50 km of the shore; thus, reliable wind data sources for coastal regions are needed. When predicting wind energy production, an accurate estimation of the wind speed distribution is of essential importance as the wind power output is proportional to the cubed wind speed. Although the offshore wind resources in the North and the Norwegian Sea have previously been assessed, to the best of our knowledge, the wind resources in the Barents Sea have not been addressed in the existing literature.

This paper aims to evaluate the suitability of the Sentinel-1 OWI component for near-surface offshore wind energy assessments. We compared it to in situ measurements and three reanalysis products: the global reanalysis ERA5 and the regional reanalyses CARRA and NORA3, within a one-year case study for the Goliat station in the Barents Sea, presenting a comprehensive assessment of wind data sources available for the Norwegian Arctic offshore region. Wind data were compiled from all sources for the year 2022 and a statistical analysis was performed. This study is of particular interest to GoliatVIND, a floating offshore wind demonstration project currently in the planning stage that will be located near Goliat to supply renewable energy to the oil platform, reducing its carbon emissions [4].

The paper is organized as follows: Section 2 provides the theoretical background containing relevant research. Section 3 presents the utilized wind datasets and applied analysis methodology. Section 4 provides the results and discussion. Finally, the conclusions are presented in Section 5.

## 2. Theoretical Background

### 2.1. Reanalysis Products

Reanalysis data are produced by assimilating historical weather observations into a numerical weather prediction (NWP) model. The reanalysis datasets that are publicly available are often characterized by a low spatial resolution, typically ranging from 3 to 50 km. ERA5, CARRA, and NORA3 have each been validated against observations in previous studies.

Although ERA5 performs well in offshore areas and has been shown to generally outperform other global reanalysis products, its low spatial resolution of 31 km causes a significant performance decrease in coastal areas due to the changes in surface roughness and topology not being discernible in the dataset [2]. This is important in the coastal areas of northern Norway, where the complex mountainous coastlines and fjords can produce intricate wind fields that extend far out over the ocean. In Figure 1, where the wind comes from inland, this is evident in the long black shadows in the Sentinel-1 backscatter caused by the complex terrain. Beyond that, the low spatial resolution of ERA5 restricts its ability to adequately resolve mesoscale features. Several studies illustrated the weaknesses of ERA5 in the representation of weather phenomena characteristic to the Arctic climate system, such as polar lows, which would have a considerable effect on potential wind farms due to the occurring high wind speeds [5,6].

Reanalysis products generally exhibit the tendency to underestimate mean wind speed as compared to in situ measurements. The strongest tendency for the reanalysis products utilized here was found for ERA5 [3]. While this underestimation seems to be proportional to the ruggedness of the terrain, it is still present for terrain with low ruggedness, e.g., the ocean surface. In addition, a negative correlation of this underestimation with latitude was found. Both of these results reduce the impact of this tendency on the Norwegian Arctic offshore region. Regional reanalysis products tend to be more adequate to represent

smaller-scale and region-specific weather events and the spatial and temporal variability of wind. This was shown to be the case for both CARRA and NORA3; although a slight underestimation of mean wind speed was still found, they improved the representation of the spatial variability, temporal variability, and climatology of extremes in both offshore and coastal regions [5–7]. For both regional reanalysis products, a substantial part of the improvements compared to ERA5 were attributed to the higher spatial resolution.

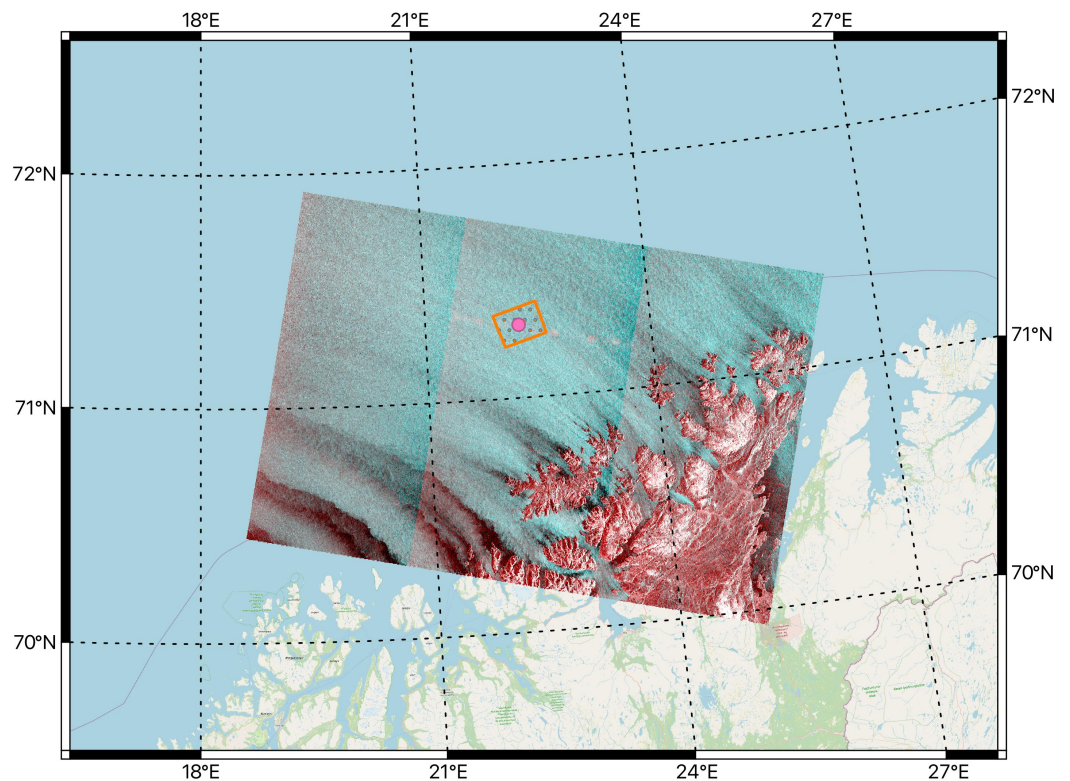


**Figure 1.** Illustration of the geographical area investigated in this study. The Goliat station (pink dot), located in the Barents Sea, 85 km north of Hammerfest; the search polygon for SAR data (orange rectangle); and false-color composite representation (HH, HV, and HV polarizations as RGB) of Sentinel-1 SAR images for 3 January 2022. The false-color composite scene illustrates the intensity of the backscatter in dB, where higher values, i.e., bright areas, correspond to the rougher surface and, therefore, higher wind speed, and darker areas correspond to a smooth ocean surface and, thus, lower wind speed.

## 2.2. Sentinel-1 Level-2 OWI Product

Wind data retrieval from satellite observations offers valuable complementary insights into offshore wind resources. Although a number of studies have attempted to utilize satellite scatterometers for offshore wind energy assessment, their low spatial resolution provides no advantage over reanalysis products [8]. SAR is capable of producing near-surface offshore wind speed data with a grid size of 1 km, a significantly higher resolution than all reanalysis products presented here. SAR operates at a variety of characteristics, such as frequency bands, polarization channels, and spatial resolutions, and responds to dielectric properties, geometry, and roughness, and to an object's surface or volume structure, depending on the penetration depth of the signal. One of the most crucial advantages of this type of sensor is the complete independence of solar illumination and weather conditions due to wavelengths that can penetrate dense clouds [9]. This is especially important for polar areas since dense cloud cover and long periods of darkness prevail there for several months of the year.

Wind speed can be estimated from SAR sensors through the measurement of the backscatter of the sea surface. As capillary waves and, thus, sea surface roughness, are directly dependent on atmospheric forcing, the sea backscattering in the C-band can be understood as a function of wind speed, wind direction (relative to the look angle), and incidence angle. However, other influences such as oil slicks, strong surface currents, or reflection from nearby coastlines can distort this proportionality. Furthermore, different polarization signals inhibit different limitations in the accurate representation of either low or high wind speeds: while co-polarized signals saturate with increasing wind speeds, cross-polarized signals cannot be distinguished from instrument noise at low wind speeds. Even a combined signal wind retrieval approach requires a priori information about the wind direction most commonly provided by NWP models [10]. Lastly, as no information about atmospheric stratification is available, wind retrieval at 10 m above the surface from SAR utilizes a geophysical model function assuming neutral stability. Therefore, the method cannot respond to changes in wind speed due to atmospheric stratification [11].

The key limitation of wind products acquired from SAR technology is its temporal resolution. Therefore, even when collecting a long time series, SAR cannot provide the same amount of temporal information as reanalyses or in situ observations. Barthelmie and Pryor conducted a detailed study assessing the suitability of limited satellite time series data for estimating the stochastic parameters of the wind speed distribution [12]. They showed that when accepting an uncertainty of  $\pm 10\%$  at a confidence level of 90%, only 150 (randomly selected) scenes are required to characterize both the mean wind speed and the variance sufficiently accurate. However, in the case of Sentinel-1, the scenes are not randomly selected but exhibit a strong temporal selectivity, as the satellite revisits any specific area only at certain times of the day. This provokes a discussion of the diurnal variability present in the investigated wind fields. Although coastal areas exhibit diurnal cycles largely due to advective effects, no strong diurnal patterns are expected over the open ocean.

To the best of our knowledge, the Sentinel-1 Level-2 OWI component has only been assessed in a small number of case studies, each comparing it to in situ observations, e.g., around Ireland [8], around Cyprus [13], and in the Ionian Sea [14]. Similar to the reanalyses, a tendency of the Sentinel-1 OWI component to underestimate wind speed was found, where the bias linearly decreased with increasing wind speed. When estimating average wind power, the errors as compared to results obtained from in situ measurements were between 5 and 10%. However, none of these studies compares the Sentinel-1 data to the reanalyses, which are more commonly used for wind resource assessments than in situ observations. Off the coast of Norway, where measurement stations are especially sparse and the complex coastlines produce intricate wind field patterns, this intercomparison will be of great value for the future of wind resource assessments, further reducing project risk at the site-finding stage.

### 3. Methods

#### 3.1. Datasets

In this study, five different wind speed and wind direction data sources were analyzed: in situ observations, three reanalysis products, including one global reanalysis product and two regional reanalysis products, and a SAR-based remote sensing product. The following subsections briefly present the technical details of each data source used for the analyses. Table 1 displays the datasets used in this study along with the main characteristics and their crucial differences.

**Table 1.** List of datasets used in this study along with their crucial characteristics. Even though in situ observations have a high spatial resolution, the singular point corresponds to a certain small area (point on a map), which does not allow any further information about the broader surrounding area to be obtained.

Dataset	Type	Resolution	
		Temporal	Spatial
Seklima	in situ observation	every 20 min	singular point
ERA5	Global reanalysis	hourly	31 km
NORA3	Regional reanalysis	hourly	3 km
CARRA	Regional reanalysis	every 3 h	2.5 km
Sentinel-1	SAR-based	once in 1–2 days	1 km

### 3.1.1. In Situ Observations

For this study, measurements provided by the Norwegian Center For Climate Services (Seklima) were used, particularly from a single Norwegian offshore station, Goliat Fpso (Station number: SN76956; Goliat), located in the Barents Sea (71.31° N, 22.25° E) [15]. The sensor is located 46 m above mean sea level and has been operating from 9 September 2015. It provides wind speed and wind direction information, extrapolated to 10 m.a.s.l. by employing a power law wind profile with a wind shear coefficient of 0.13 [16]. From all data sources investigated in this study, this method has the highest temporal resolution, providing measurements every 20 min, averaged over 10 min intervals.

As Figure 1 illustrates, the wind field around and at the Goliat station is influenced by the complex coastline if the wind comes from inland. The sea surface at this location is not expected to be affected by wave reflections off the coast, rendering this a suitable place for comparison. However, it also limits the applicability of the results of this study to areas closer to the shore or even within fjords. This specific location was recently selected for the construction of an offshore wind farm. Thus, comparing the measurement data from this site with other available wind data sources can provide unique complementary insights into the design and implementation of wind power, not only for the Goliat station, but also for future offshore wind power exploitation in general.

### 3.1.2. Reanalyses

#### ERA5

ERA5 is the fifth-generation global reanalysis model developed by the European Centre for Medium-Range Weather Forecasts (ECMWF) [17]; it is publicly available through the Copernicus Climate Change Service. It has a spatial resolution of approximately 31 km, rendering it unable to resolve mesoscale features and complex topology along coastlines. Its temporal resolution, however, is very high, providing instant values of hourly wind speed and direction. In this study, we used the “10 m u-component of wind” and “10 m v-component of wind” from the ERA5 hourly data on single levels, calculating the wind speed via  $\sqrt{u^2 + v^2}$  [18].

#### NORA3

NORA3 is a regional reanalysis model produced by the Norwegian Meteorological Institute covering the North Sea, the Norwegian Sea, and the Barents Sea (44.02° N–84.06° N, 30.17° W–85.79° E) with a spatial resolution of 3 km. The NORA3 data are obtained by downscaling ERA5 data using a nonhydrostatic convection-permitting numerical weather prediction model (HARMONIE-AROME) [19]. Along with the wind field, NORA3 provides various atmospheric and surface meteorological parameters, such as mean sea level pressure, air temperature and relative humidity, fog, wind speed, and direction [20]. Solbrekke et al. demonstrated that the wind field in NORA3 is much improved relative to its

host analysis, particularly in mountainous areas and along the improved grid-resolving coastlines. In this study, we used NORA3 as one of the reanalysis sources since it is specifically designed and validated for Norway and has a high spatial and temporal resolution, providing instant values of wind speed and direction at 10 m.a.s.l. for every hour.

### CARRA

CARRA (Copernicus Arctic Regional Reanalysis) was the second regional reanalysis product used in this study. It contains 3-hourly analyses along with hourly short-term forecasts at a 2.5 km resolution of atmospheric and surface meteorological parameters, such as surface and near-surface temperature, precipitation, humidity, wind, pressure, and atmosphere fluxes. It is divided into CARRA-East and CARRA-West; the west domain covers Greenland along with the neighboring seas and territories. In this study, we were interested in the East domain, which covers Svalbard, Franz Josef Land, Novaya Zemlya, and the northern parts of Scandinavia [21]. Similar to NORA3, CARRA was also created by the HARMONIE-AROME with the ERA5 global reanalysis as lateral boundary conditions. In addition, some enhancements have been implemented in comparison to both ERA5 and the operational HARMONIE-AROME modeling systems, including extensive utilization of satellite data for the HARMONIE-AROME operational weather prediction system, significant augmentation in the surface observation datasets, and substantial improvements in the regional physiography and orography [7]. Furthermore, CARRA utilizes an improved data assimilation system compared to NORA3.

#### 3.1.3. Remote Sensing

The OWI component from the Sentinel-1 Level-2 OCN product was acquired through the publicly available Copernicus Open Access Hub, the European Union's Earth observation program. Sentinel-1 operates at the C-band with a central frequency of 5.404 GHz and includes two polar-orbit Sentinel-1A and Sentinel-1B missions that provide multiple sensing modes, such as stripmap (SM), extra-wide (EW), wave (WV), and interferometric-wide (IW) swath modes in single (HH or VV) or dual polarization (HH + HV or VV + VH) at a 40 m spatial resolution. SAR reaches equilibrium within less than one minute. The Sentinel-1 Level-2 OCN OWI component is fully calibrated and is provided as an ocean surface wind vector, including wind speed and wind direction, estimated from Sentinel-1 Level-1 SAR images by inversion of its associated normalized radar cross section (NRCS). It is a ground range gridded estimate of the surface wind speed and direction at 10 m above the surface with a spatial resolution of 1 km.

In this study, we focused on the extraction of the available Sentinel-1 Level-2 OCN scenes for the Goliat station for 2022. For Northern Norway, the acquisition mode is IW, which is acquired using the TOPSAR technique, providing an improved quality product by enhancing image homogeneity. Sentinel-1 revisits the region of interest of this study once every 1–2 days, passing either at around 5:00 UTC or 16:00 UTC.

#### 3.2. Temporal and Spatial Preprocessing

The 238 SAR scenes available from Sentinel-1 between January and December 2022 for the area covering the Goliat station were extracted, providing wind speed and direction information at 10 m above the ocean surface. Subsequently, the same information from all the above-mentioned data sources, including the Seklima in situ observations and the three reanalyses ERA5, CARRA, and NORA3 were acquired, overlapping with the Sentinel-1 data both spatially and temporally. In the case of low-resolution ERA5, this matchup was performed by extracting the single point of the output grid closest to the Goliat station. For CARRA, NORA3, and Sentinel-1, which have higher spatial resolutions, the mean value of the four closest points was computed. The Seklima data were employed as the reference source, as in situ measurements are commonly assumed to provide the most accurate observations.

The data sources differ in temporal and spatial resolution. The Seklima data have the lowest spatial resolution (singular) and highest temporal resolution, providing the wind speed and direction data every 20 min. The global ERA5 reanalysis provides wind data at a low spatial resolution (31 km); however, it has a high temporal resolution with data provided every hour. On the other hand, CARRA reanalysis has a significantly higher spatial resolution (3 km), but relatively lower temporal resolution (3 h). The optimal source from both spatial and temporal resolution points of view is NORA3 with a spatial resolution of 3 km, which is provided hourly. Sentinel-1 provides wind produce with the highest spatial resolution (1 km), but at the expense of temporal resolution, with a maximum of one scene per day.

### 3.3. Statistical Analysis

In order to properly compare the differences between all the above-mentioned wind data sources, and to quantitatively evaluate the accuracy of the Sentinel-1 SAR-based wind speed and direction product, we applied several commonly employed stochastic measures to the full datasets, such as root mean squared error (RMSE), Pearson correlation coefficient, and standard deviation [22]. RMSE is one of the most commonly used measures for evaluating the quality of forecasts/predictions. It illustrates the deviation of a prediction from the reference value for each point of a time series by calculating the Euclidean distance between the two. The Pearson correlation coefficient captures the amount of linear correlation between two variables, ranging from  $-1$  to  $+1$ . The standard deviation displays the spread of the data points around the mean value from the dataset, thus showing the dispersion in a set of values.

### 3.4. Wind Speed Distribution

The stochastic character of wind speed allows its representation by a probability density function. For the assessment of offshore wind resources in a given region, an accurate representation of the wind speed distribution is crucial. The Weibull distribution  $f(v, \lambda, k)$  is widely used for this purpose as it generally provides a good fit to offshore wind speed data [23]:

$$f(v, \lambda, k) = \frac{k}{\lambda} \left(\frac{v}{\lambda}\right)^{k-1} \exp\left(-\left(\frac{v}{\lambda}\right)^k\right) \quad (1)$$

with the wind speed  $v \in \mathbb{R}^+$ , the scale parameter  $\lambda > 0$ , and the shape parameter  $k > 0$ . The scale parameter  $\lambda$  specifies the ratio of horizontal to vertical extent of the distribution, i.e., an increase in  $\lambda$  results in a wider and lower Weibull distribution. The shape parameter  $k$  indicates the skewness of the distribution; a larger value for  $k$ , therefore, indicates more frequent high-wind-speed events. In a continuation of their work, Pryor et al. evaluated the critical sample size of independent SAR scenes needed to characterize the Weibull parameters. They came to the conclusion that no more than 250 observations are needed for an uncertainty of  $\pm 10\%$  at a confidence level of 90% for the characterization of both Weibull parameters [24].

For an estimation of the annual wind power production of a wind turbine at a given site, the wind speed would first have to be extrapolated vertically to the hub height of the turbine. There are a number of models commonly used for this purpose, each with its own limitations. In heterogeneous terrain, models such as the logarithmic law or the power law are recognized as applicable well up to heights of 200 m and 300 m above the ground, respectively [25]. However, as wind turbines are rapidly increasing in size, especially offshore and for floating foundations (e.g., the Vestas V236-15.0 MW model by Vestas Wind Systems A/S in Aarhus, Denmark reaches a rotor diameter of 236 m), and as the atmospheric boundary layer above the smooth ocean surface is much shallower than over complex or rough terrain, the case discussed in this study extends far beyond the applicability of these models. More complex models require knowledge about many more atmospheric parameters that were not available to us for the considered location. Therefore, in this study, we limit the analysis of the available wind power to the comparison of the

Weibull distributions fitted to the 10 m wind speed histograms of each data source, as the wind speed distribution and wind power output are closely related. Although it is outside of scope of this study, the authors note the necessity to explore this issue further and find alternative solutions in order to maintain the performance of offshore wind resource estimation in the future.

## 4. Results and Discussion

### 4.1. Wind Speed

As the wind power available at a given site is proportional to the cubed wind speed, a precise assessment of the wind speed distribution and of the uncertainty present in the available data is of critical importance for wind energy purposes. It is a crucial parameter that directly impacts wind energy potential, influences the capacity factor and profitability of a given location, and affects the choice of wind turbine. Since wind turbines are optimized for particular wind speed ranges, the wind speed distribution present at a given site plays a key role in the selection of the turbine type. Wind turbines used for offshore power production usually have a cut-in wind speed at 2–3 m/s (at hub height), a rated wind speed of 14–16 m/s, and a cut-off wind speed between 25 and 30 m/s. Therefore, the interval ranging from the cut-in to the cut-off wind speed, and especially between the cut-in and the rated wind speed, has to be represented with high accuracy for wind power assessment purposes. It is worth noting that, as most wind data sources provide the wind speed at 10 m above the ocean surface, the wind speed interval of interest is shifted relative to that at the hub height.

#### 4.1.1. Scatterplots

Figure 2 shows scatterplots obtained from comparing the wind speed from the reference source, i.e., Seklima in situ observations, to each other source, including ERA5, NORA3, and CARRA reanalyses, and Sentinel-1. The Seklima data are plotted on the horizontal axis, all other sources are plotted along the respective vertical axes. The background heatmaps provide extra insight into the distribution of wind speed across the scatterplot. Accordingly, darker regions in the heatmap signify a higher density of data points. The scatterplots clearly demonstrate a very strong positive linear relationship between all pairs of datasets shown. The close clustering of data points suggests a strong similarity between the Seklima dataset and all three reanalyses, and between Seklima and the Sentinel-1 data. Linear regressions were fitted to each scatterplot, with the slope and intercept parameters varying only slightly between data sources.

#### 4.1.2. Statistical Metrics

In order to quantitatively evaluate the statistical differences between the above-mentioned sources, a number of metrics, including RMSE, Pearson correlation coefficient, and standard deviation, were calculated for Sentinel-1, ERA5, NORA3, CARRA, each with respect to Seklima. Table 2 presents the results, while Figure 3 shows the Taylor diagram, visualizing all the above-mentioned metrics for all data sources in a single plot.

**Table 2.** Statistical metrics applied to wind speed time series from each data source compared to the reference source, Seklima, in situ observations.

Dataset	RMSE [m/s]	Correlation Coeff.	Std. Deviation [m/s]
<b>Seklima</b>	-	-	4.19
<b>ERA5</b>	1.65	0.92	3.82
<b>NORA3</b>	1.80	0.90	3.98
<b>CARRA</b>	2.05	0.88	4.03
<b>Sentinel-1</b>	2.00	0.88	3.95

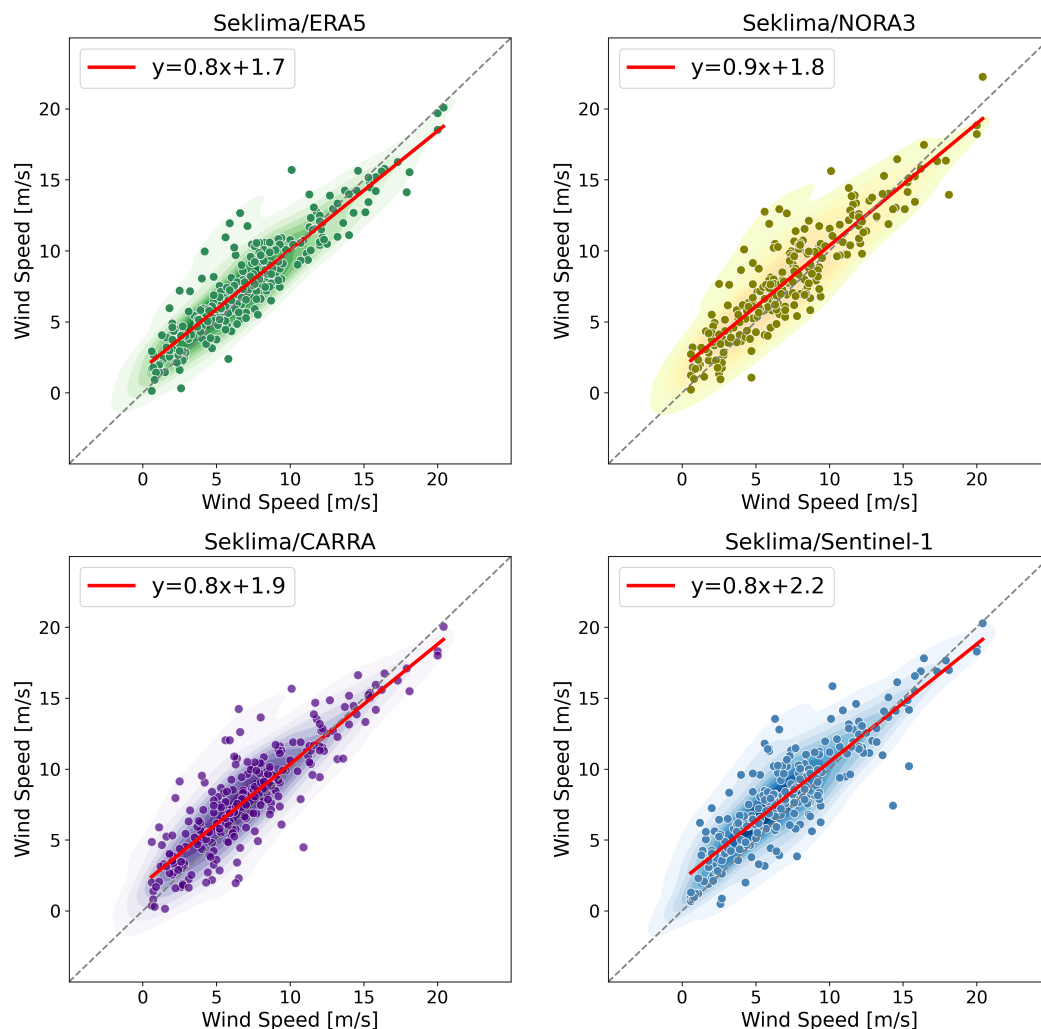


**Figure 2.** Scatterplots of wind speed data from Seklima (plotted on the horizontal axes) versus ERA5, NORA3, CARRA, and Sentinel-1 (plotted on the respective vertical axes).

The RMSEs of the four data sources ranged from 1.65 m/s to 2.05 m/s. ERA5 had the lowest RMSE with 1.65 m/s, indicating a slightly more accurate model compared to those with higher RMSEs, namely, CARRA with a maximum value of 2.05 m/s. Despite the range, it is worth noting that all four data sources had relatively close RMSE values, demonstrating similar levels of accuracy. Moreover, we can highlight that the RMSE of Sentinel-1 fell within the range of RMSE values obtained for the three reanalyses, displaying a similar closeness between the respective wind speed time series. The Pearson correlation coefficient ranged between 0.88 for both CARRA and Sentinel-1 and 0.92 for ERA5, again placing the SAR-based data within the values obtained for the three reanalyses, and indicating a high overall correlation with the reference data. While the scatterplots only visually demonstrated the relationship between the Seklima data with the Sentinel-1 and the reanalyses data, the correlation coefficient confirmed that there was a strong linear relationship between the compared sources and the reference data. Table 3 displays the cross-correlation between the wind speed data sources. This specifically demonstrates the close relationship between the global reanalysis ERA5 and the two regional reanalyses CARRA and NORA3. This likely results from CARRA and NORA3 employing ERA5 as their host model.

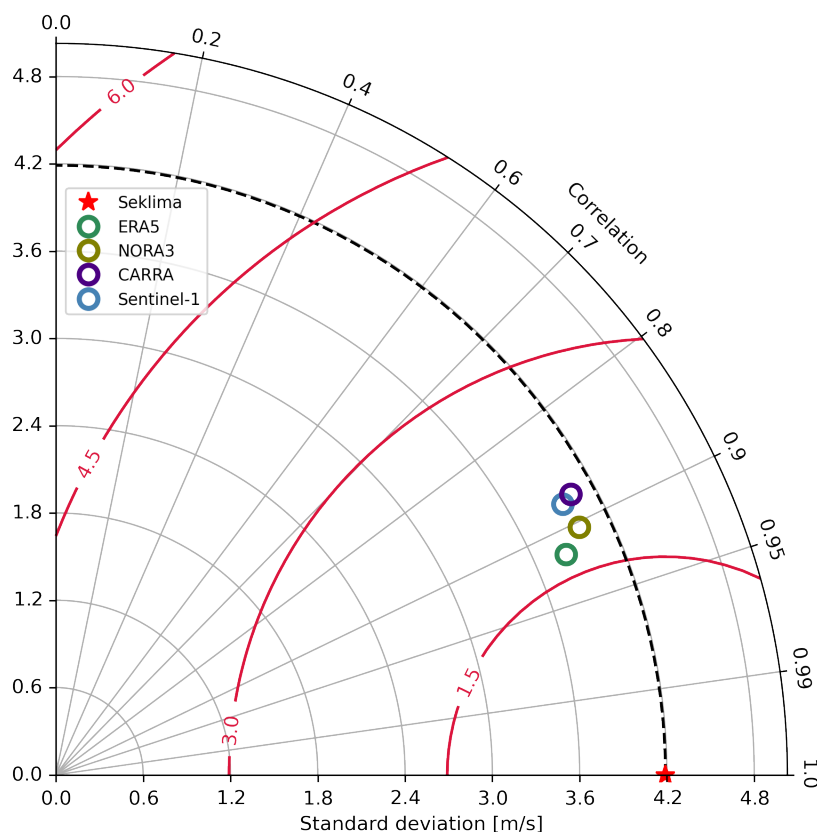


**Figure 3.** Taylor diagram for wind speed data from Seklima versus ERA5, NORA3, CARRA, and Sentinel-1. The red contours display the RMSE value of the data sources compared to the reference source.

**Table 3.** Cross-correlation matrix between the different wind speed data sources, i.e., Seklima, ERA5, NORA3, CARRA reanalysis, and Sentinel-1.

Variables	Seklima	ERA5	NORA3	CARRA	Sentinel-1
Seklima	1	0.92	0.90	0.88	0.88
ERA5		1	0.98	0.93	0.91
NORA3			1	0.94	0.91
CARRA				1	0.88
Sentinel-1					1

The reference data (Seklima—red star) had a higher standard deviation than all other sources, indicating the largest amount of wind speed variability. This is interesting as it is the only source that averages its output values over a longer time interval (10 min); all other sources provide instantaneous or pseudo-instantaneous values. Since shorter sampling periods lead to higher gusts being captured in the data as compared to long averaging periods, the difference in averaging periods present in the data sources investigated within this study could have led to the hypothesis that the reanalyses and the Sentinel-1 data display a higher wind speed variability, and thus, variance. The contrary seems to be the case here, as none of the other data sources were able to fully capture the wind speed variance displayed by the in situ observations; all other data sources had a slightly lower standard deviation than Seklima. ERA5 had the lowest standard deviation of 3.82, thus representing the least amount of variability in wind speed. Nevertheless, it should be noted that the standard deviation did not range significantly among the five data sources, which implies a similar variation of values among the datasets.

#### 4.1.3. Wind Speed Occurrences

Figure 4 shows histograms of the differences in wind speed occurrences acquired by several sources between the reference source, Seklima, and the other data sources, namely, ERA5, NORA3, CARRA, and Sentinel-1. The horizontal axis represents the range of wind speeds in m/s, while the vertical axis displays the difference of wind speed occurrence in percent. Accordingly, when the occurrence frequency difference is 2, it shows that the corresponding wind speed occurred 2% more often in the reference data than the compared source. Moreover, each histogram displays the maximum, minimum, and variance of the differences.

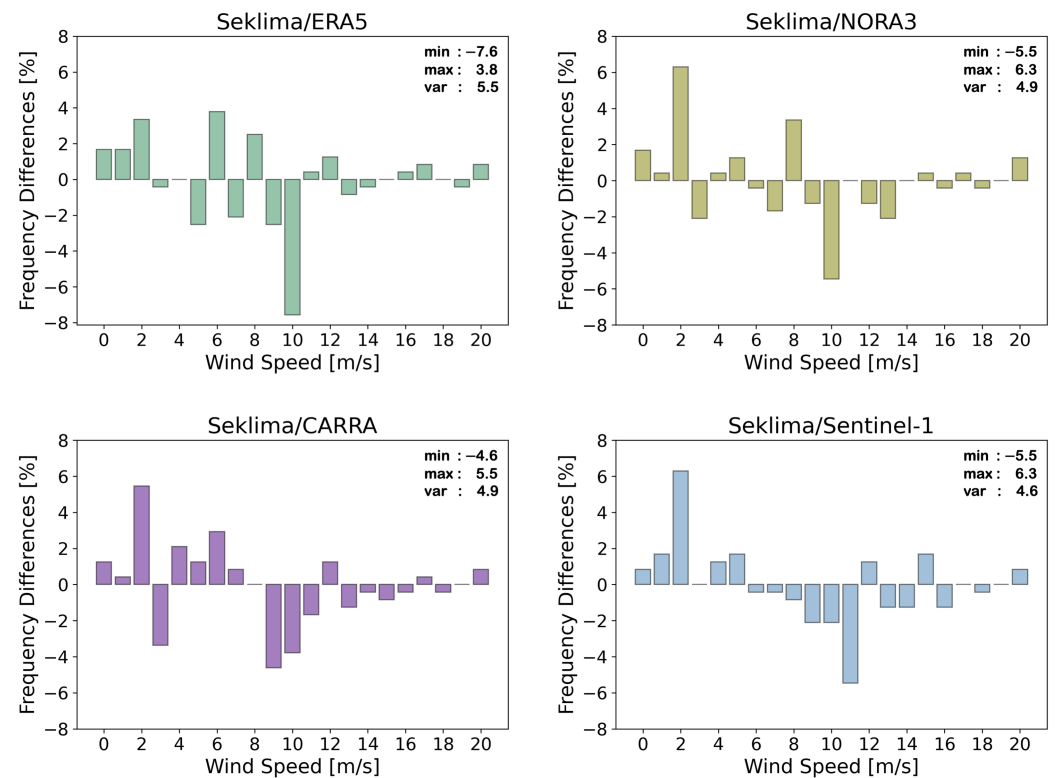


**Figure 4.** Histograms of the differences in wind speed occurrences between Seklima and the other data sources, i.e., ERA5, NORA3, CARRA reanalysis, and Sentinel-1.

Most of the wind speed differences fell within the range of  $-2$  to  $+2\%$ , suggesting a good level of agreement for those wind speed intervals. However, for all data sources, there were higher values of disagreement present, both on the positive and negative side. Generally, the outliers tended to be either consistently positive or negative throughout all combinations of data sources, indicating a similar bias present in all reanalyses and the Sentinel-1 data as compared to the in situ measurements. All sources displayed an under-representation of the 2 m/s wind speed, which might correspond to difficulties in capturing low-wind events. The most significant over-representation was detected for wind speed values around 9–11 m/s.

Another interesting point is that Sentinel-1 had the lowest variance in wind speed difference among all the sources, which means that the data points were relatively consistent and indicated a higher level of accuracy in the wind speed prediction than other sources. On the other hand, ERA5 provided the highest variance, which means that the spread of the values was larger and the wind speed precision might not have been very consistent. However, it should be mentioned that the variance differences were small between the sources, with the highest variance equal to 5.5 (ERA5) and the lowest to 4.6 (Sentinel-1).

The histograms provide valuable insight into the reliability and consistency of wind speed data obtained from different sources by highlighting intervals that are in need of

further calibration. Overall, they give rise to the impression that all reanalyses and the SAR-based product tended to underestimate low wind speeds and overestimate high wind speeds as compared to the in situ observations that were employed as reference data. It should be noted that these discrepancies do not necessarily indicate a bad performance of the reanalyses or the Sentinel-1 product; the fact that there were differences similar in tendency and magnitude that were consistent for all compared data sources suggests that there might have been a bias present in the in situ measurement data. As a matter of fact, a study investigating vertical wind profiles for nine oil platforms in the south of Norway concluded that the power law with a wind shear coefficient of 0.13 that is presently employed on Norwegian oil platforms results in an average 0.8 m/s underestimation of the 10 m wind speed [16]. As these observations are, in turn, used for the assimilation and verification of reanalysis products, these findings highlight the need for a more independent, yet accurate representation of the wind speed distribution.

#### 4.2. Wind Direction

Another important parameter in the preliminary site assessment for wind energy purposes is wind direction. Along with wind speed, it plays a fundamental role in optimizing the wind energy generation of a given wind farm. In particular, information about the distribution of the wind direction significantly influences the wind park layout and, thus, aids in maximizing the energy output by avoiding wake losses within the wind farm. Furthermore, the complex topology of the fjords and mountains in the coastal areas of Northern Norway heavily affects the wind field over the ocean, as can clearly be seen in Figure 1. In order to choose the optimal location, a high spatial resolution capable of resolving the intricate wind patterns present in these areas is essential.

Figure 5 shows the wind roses of all data sources, displaying the occurrences of wind directions and a rough representation of the wind speed distribution for each wind direction bin, allowing for a visual comparison between sources. Overall, all diagrams display similar prevailing wind directions, namely, mainly from the East and West South West. Some differences are discernible, e.g., the wind direction distribution of ERA5 seemed to fluctuate less than all other data sources, which may result from its low spatial resolution and account for its inability to resolve the flow over the complex topology of the coastline nearby. Furthermore, while Sentinel-1 represented the West wind best, its representation of the wind coming from the East quartile was broader than that of Seklima and the two regional reanalyses. However, more detailed and quantitative analyses would be needed in order to properly assess the performance of the four data sources in capturing the distribution of wind direction.

#### 4.3. Wind Speed Weibull Distribution Comparison

The importance of an accurate representation of the wind speed distribution has already been discussed in this study. In order to assess the ability of the SAR-based product to capture the stochastic properties of the wind speed despite its low temporal resolution, a comparison of the sparse match-up datasets of the reanalyses and in situ observations with their respective dense datasets, that is, with their full temporal resolution, is appropriate. The first row of Figure 6 shows the wind speed histograms of the dense and the sparse Seklima data, and the Sentinel-1 data, alongside their respective Weibull distribution. The histograms and Weibull distributions of the three reanalysis products, dense and sparse, are shown in the second and third row, respectively. Additionally, Table 4 summarizes the corresponding Weibull parameters obtained for the dense and sparse wind speed datasets from all sources. The Weibull distribution obtained from the dense Seklima data was reproduced in all other plots as a reference.

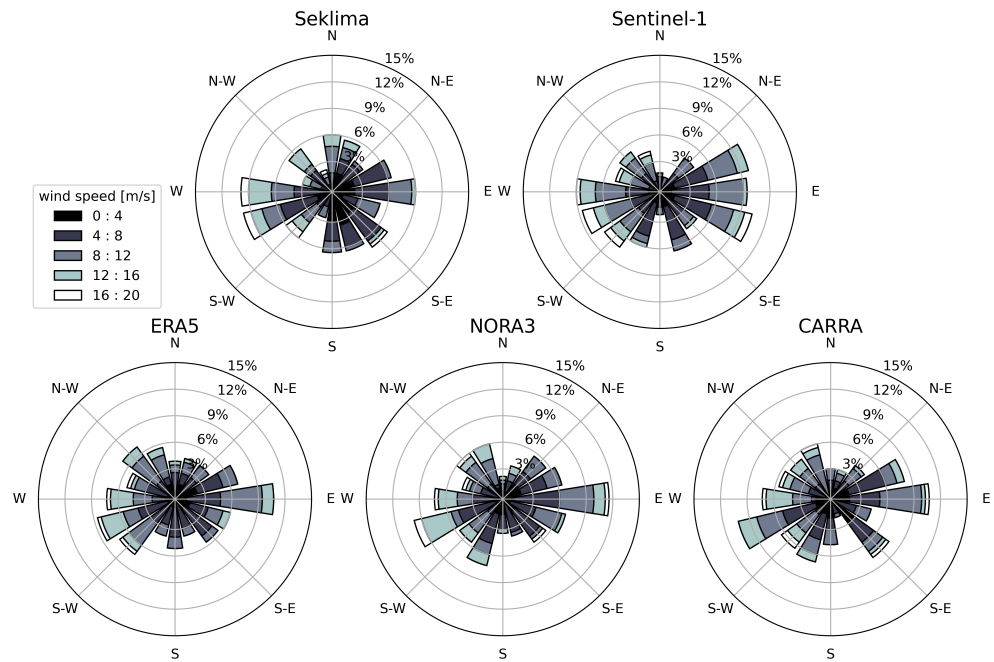


**Figure 5.** Wind roses compiling the wind direction distributions from the Seklima, ERA5, NOR3, CARRA, and Sentinel-1 datasets.

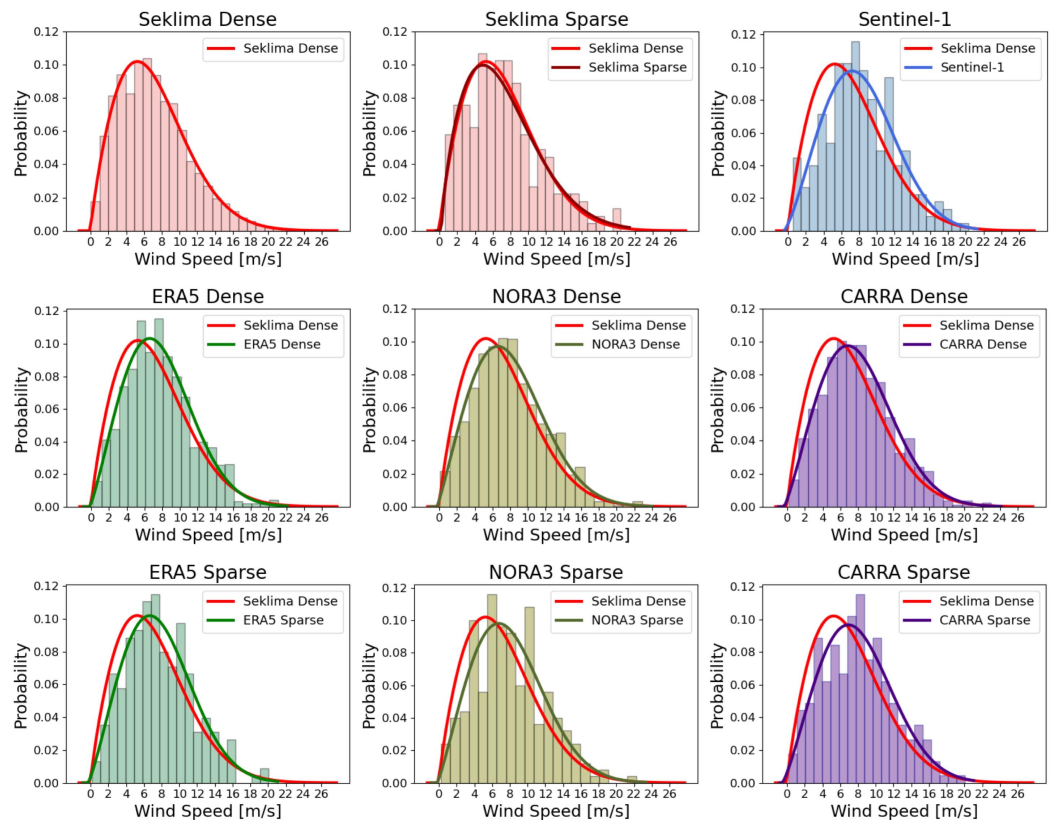


**Figure 6.** Weibull probability density function and observed wind speed histograms for several cases: dense and sparse datasets from Seklima, ERA5, NOR3, and CARRA, and Sentinel-1. *Dense* refers to the sample obtained for the Goliat station over the year 2022 with the respective full temporal resolution, that is, every 20 min for Seklima, and several times a day for the three reanalysis sources. *Sparse* refers to the subsets of the 238 data points overlapping temporally with the Sentinel-1 scenes.

**Table 4.** The Weibull shape and scale parameters  $k$  and  $\lambda$  obtained for the dense and sparse wind speed datasets from all sources.

Dataset		Weibull Parameters	
		$k$	$\lambda$
Seklima	dense	1.85	8.01
	sparse	1.70	7.83
ERA5	dense	2.21	8.90
	sparse	2.23	9.08
NORA3	dense	2.14	9.22
	sparse	2.17	9.23
CARRA	dense	2.22	9.43
	sparse	2.26	9.67
Sentinel-1	(sparse)	2.33	9.79

The Weibull parameters obtained for the Sentinel-1 dataset are  $k = 2.33$  and  $c = 9.79$ , clearly illustrating an overestimation of the distributed wind speed compared to the reference data. This result strongly contrasts with those obtained in previous studies (see Section 2), concluding that, for other specific regions, Sentinel-1 and the reanalysis products generally tended to underestimate wind speed as compared to the in situ observations. However, as discussed previously, Olsen et al. found that wind speed data obtained from measurements at Norwegian oil platforms tended to underestimate wind speed due to a flawed vertical wind profile [16]. This provides a valid explanation for the discrepancy found here. This assumption is supported by the fact that the Weibull parameters of all three reanalysis products were not just close to one another, but also very close to those of the Sentinel-1 dataset.

Although there is a visible difference between the dense and the sparse Seklima histogram, their Weibull distributions were still considerably close. The change in shape and scale parameters from the dense to the sparse sample was  $k = 1.85 \rightarrow 1.70$  (a decrease of  $\sim 8.1\%$ ) and  $\lambda = 8.01 \rightarrow 7.83$  (a decrease of  $\sim 2.25\%$ ), respectively. The differences between parameters for the dense and sparse reanalysis datasets were even less for all three reanalyses (no more than a 2% change in  $k$  and 2.5% in  $\lambda$ ). Pryor et al. determined that around 250 independent scenes are needed to characterize these parameters [24]. With these results achieved using 238 scenes, we are pleased to note that in this case, the temporal selectivity due to the sampling rate of Sentinel-1 did not seem to introduce a major bias into the distributions.

However, minor tendencies are observable. With decreasing temporal resolution, both  $k$  and  $\lambda$  decreased for Seklima but slightly increased for all three reanalysis products. For the latter, going from the dense to the sparse datasets, this resulted in lower and wider distributions with more pronounced tails and, thus, a higher mean wind speed. The opposite happened to the Seklima data; the distribution became slimmer and slightly less skewed, resulting in a lower mean wind speed. Thus, moving from the dense to the sparse datasets accentuated the discrepancy between the Seklima distribution and the four others. However, the relative changes of both  $k$  and  $\lambda$ , especially for the reanalysis products, were too small to be attributed to a potential bias resulting from temporal selectivity.

In the context of wind resource assessment, these results are valuable, but not enough. The average wind power of a site with a certain wind speed Weibull distribution is given by

$$P = \frac{1}{2} \rho \lambda^3 \Gamma\left(1 + \frac{3}{k}\right) \quad (2)$$

with the gamma function  $\Gamma$  [24]. The high order of the scale parameter  $\lambda$  explains why the accuracy achieved by the number of SAR scenes used here is insufficient to characterize

the annual average wind power. According to Barthelmie et al., almost 2000 independent scenes are required to achieve an uncertainty of  $\pm 10\%$  at a confidence level of 90% [12]. For the Goliat site, this translates to almost 8.5 years of SAR data, which, for the Sentinel-1 OWI product evaluated here, are not yet available.

## 5. Conclusions

The presented analysis justifies the application of the Sentinel-1 OWI component for offshore wind resource evaluation. We found that the RMSE, correlation coefficient, and standard deviation were similar for all data sources, placing the performance of the SAR-based wind retrieval within the range of the three reanalysis products. An analysis of the wind speed differences displayed a clear bias between the in situ measurements and the other four data sources, which may result from an underestimation of the reduced wind speed as distributed from Norwegian oil platforms [16]. A qualitative review of the distribution of wind direction showed no distinct discrepancies between the data sources.

The analysis of the Weibull distributions fitted to each dataset led to a similar conclusion: while the Weibull parameters of the three reanalyses and the Sentinel-1 data were reasonably close to one another, those of the Seklima data differed considerably, resulting in a shift of the Weibull distribution towards lower wind speed values. The sparse reanalysis datasets, consisting of 238 points matching up with the SAR scenes, were compared with their respective dense datasets, containing their full temporal resolution. The change in Weibull parameters between the two variants was no more than 2.5% for both scale and shape parameters. This suggests the conclusion that the low temporal resolution of the Sentinel-1 data is not generally an obstacle in the accurate representation of the wind speed distribution. However, in order to perform a complete wind resource assessment with a reasonable accuracy, a longer time series would be required. Nonetheless, its unmatched spatial resolution renders it a valuable source of information for wind resource assessments in offshore areas affected by complex coastlines unresolved by other data sources. Furthermore, it offers the potential to resolve mesoscale features such as polar lows, which are often not captured by reanalysis products.

This study analyzed some of the similarities and dissimilarities present in the available data sources for assessing near-surface offshore wind in the Norwegian Arctic. However, it is far from exhaustive. Future studies could include both a spatial and temporal expansion of the data taken into consideration, enabling a more accurate representation of the stochastic characteristics of all sources. In this context, several questions could be addressed that arise naturally from this work: How does the Sentinel-1 OWI component perform under varying meteorological conditions, i.e., at the tails of the wind speed distribution? How severely is it affected by the coastline when moving closer to the shore or even into fjords? And how large are the errors introduced by atmospheric stratification that deviates from the assumed neutral stability? An in-depth analysis of spatial and temporal variability, such as diurnal, seasonal, and interannual variability, would also prove valuable to further characterize the wind climatology in the Norwegian Arctic and aid in the understanding of the limitations of the Sentinel-1 OWI component for offshore wind resource assessments. Lastly, a more holistic approach to wind resource evaluation procedures has to be developed in order to utilize the added value of SAR-based wind retrieval for wind farm planning and development.

**Author Contributions:** E.K.: Conceptualization, Data curation, Formal analysis, Methodology, Visualization, Writing—original draft, Writing—review and editing. P.A.: Conceptualization, Formal analysis, Investigation, Methodology, Writing—original draft, Writing—review and editing. P.A. and E.K. contributed equally to this work. L.Z.: Conceptualization, Data curation, Writing—review and editing. Y.B.: Conceptualization, Supervision, Writing—review and editing. I.E.: Conceptualization, Supervision, Writing—review and editing. B.R.: Conceptualization, Supervision, Writing—review and editing. All authors have read and agreed to the published version of the manuscript.

**Funding:** This work is funded by Equinor Akademiaavtalen with UiT—The Arctic University of Norway. Patricia Asemann is supported by a fellowship of the German Academic Exchange Service (DAAD). Igor Esau acknowledges a contribution from the ESA project MAXSS 4000132954/20/I-NB.

**Institutional Review Board Statement:** Not applicable.

**Informed Consent Statement:** Not applicable.

**Data Availability Statement:** Publicly available datasets were analyzed in this study. Sentinel-1 SAR data is accessible on Copernicus Open Access Hub at <https://dataspace.copernicus.eu/>. ERA5 and CARRA data are available through the Climate Data Store <https://cds.climate.copernicus.eu/>, while NORA3 reanalysis is obtainable through <https://marine.met.no/>. Finally, Seklima data is available at the Norwegian Centre for Climate Services <https://seklima.met.no/>.

**Conflicts of Interest:** The authors declare no conflicts of interest.

## Abbreviations

The following abbreviations are used in this manuscript:

SAR	Synthetic Aperture Radar
OWI	Ocean Wind Field
NWP	Numerical Weather Prediction
ECMWF	European Centre for Medium-Range Weather Forecasts
SM	Stripmap Mode
EW	Extra-Wide Mode
WV	Wave Mode
IW	Interferometric-Wide Mode
NRCS	Normalized Radar Cross Section
RMSE	Root Mean Squared Error

## References

- International Energy Agency. *World Energy Outlook 2019*; International Energy Agency: Paris, France, 2019. [CrossRef]
- Gualtieri, G. Reliability of ERA5 Reanalysis Data for Wind Resource Assessment: A Comparison against Tall Towers. *Energies* **2021**, *14*, 4169. [CrossRef]
- Dörenkämper, M.; Olsen, B.T.; Witha, B.; Hahmann, A.N.; Davis, N.N.; Barcons, J.; Ezber, Y.; García-Bustamante, E.; González-Rouco, J.F.; Navarro, J.; et al. The Making of the New European Wind Atlas—Part 2: Production and evaluation. *Geosci. Model Dev.* **2020**, *13*, 5079–5102. [CrossRef]
- Source Galileo. GoliatVIND. 2023. Available online: <https://goliatvind.no> (accessed on 17 October 2023).
- Haakenstad, H.; Breivik, Ø.; Furevik, B.R. NORA3: A Nonhydrostatic High-Resolution Hindcast of the North Sea, the Norwegian Sea, and the Barents Sea. *Wind Energy Sci.* **2021**, *60*, 1443–1464. [CrossRef]
- Moreno-Ibáñez, M.; Laprise, R.; Gachon, P. Recent advances in polar low research: Current knowledge, challenges and future perspectives. *Tellus A Dyn. Meteorol. Oceanogr.* **2021**, *73*, 1890412. [CrossRef]
- Køltzow, M.; Schyberg, H.; Støylen, E.; Yang, X. Value of the Copernicus Arctic Regional Reanalysis (CARRA) in representing near-surface temperature and wind speed in the north-east European Arctic. *Polar Res.* **2022**, *41*, 8002. [CrossRef]
- de Montera, L.; Remmers, T.; O’Connell, R.; Desmond, C. Validation of Sentinel-1 offshore winds and average wind power estimation around Ireland. *Wind Energy Sci.* **2020**, *5*, 1023–1036. [CrossRef]
- Sandven, S.; Johannessen, O.M.; Kloster, K. Sea Ice Monitoring by Remote Sensing. *Encycl. Anal. Chem.* **2006**, *1993*, 1–43. [CrossRef]
- Tollinger, M.; Graversen, R.; Johnsen, H. High-Resolution Polar Low Winds Obtained from Unsupervised SAR Wind Retrieval. *Remote Sens.* **2021**, *13*, 4655. [CrossRef]
- ESA. Level 2 OCN Ocean Wind Field Component. Available online: <https://sentinels.copernicus.eu/web/sentinel/ocean-wind-field-component> (accessed on 31 August 2023).
- Barthelmie, R.J.; Pryor, S.C. Can Satellite Sampling of Offshore Wind Speeds Realistically Represent Wind Speed Distributions? *J. Appl. Meteorol.* **2003**, *42*, 83–94. [CrossRef]
- Hadjipetrou, S.; Liodakis, S.; Sykioti, A.; Katikas, L.; Park, N.W.; Kalogirou, S.; Akylas, E.; Kyriakidis, P. Evaluating the suitability of Sentinel-1 SAR data for offshore wind resource assessment around Cyprus. *Renew. Energy* **2022**, *182*, 1228–1239. [CrossRef]
- Caligiuri, C.; Stendardi, L.; Renzi, M. The use of Sentinel-1 OCN products for preliminary deep offshore wind energy potential estimation: A case study on Ionian sea. *Eng. Sci. Technol. Int. J.* **2022**, *35*, 101117. [CrossRef]
- Seklima. Norsk Klima Service Senter. Available online: <https://seklima.met.no/> (accessed on 6 September 2023).

16. Olsen, A.M.; Øiestad, M.; Berge, E.; Køltzow, M.Ø.; Valkonen, T. Evaluation of Marine Wind Profiles in the North Sea and Norwegian Sea Based on Measurements and Satellite-Derived Wind Products. *Tellus A Dyn. Meteorol. Oceanogr.* **2022**, *74*, 1–16. [[CrossRef](#)]
17. Hersbach, H.; Bell, B.; Berrisford, P.; Hirahara, S.; Horányi, A.; Muñoz-Sabater, J.; Nicolas, J.; Peubey, C.; Radu, R.; Schepers, D.; et al. The ERA5 global reanalysis. *Q. J. R. Meteorol. Soc.* **2020**, *146*, 1999–2049. [[CrossRef](#)]
18. ECMWF. ERA5 Hourly Data on Single Levels from 1940 to Present. Available online: <https://cds.climate.copernicus.eu/cdsapp#!/dataset/reanalysis-era5-single-levels?tab=form> (accessed on 6 September 2023).
19. Solbrekke, I.M.; Sorteberg, A.; Haakenstad, H. The 3 km Norwegian reanalysis (NORA3)—A validation of offshore wind resources in the North Sea and the Norwegian Sea. *Wind Energy Sci.* **2021**, *6*, 1501–1519. [[CrossRef](#)]
20. MET.NO. NORA3. Available online: <https://marine.met.no/node/19> (accessed on 18 September 2023).
21. ECMWF. Copernicus Arctic Regional Reanalysis. Available online: <https://climate.copernicus.eu/copernicus-arctic-regional-reanalysis-service> (accessed on 6 September 2023).
22. Theodoridis, S.; Koutroumbas, K. *Pattern Recognition*, 4th ed.; Academic Press, Inc.: Orlando, FL, USA, 2008.
23. Pavia, E.; O'Brien, J. Weibull Statistics of Wind Speed over the Ocean. *J. Appl. Meteorol.* **1986**, *25*, 1324–1332. [[CrossRef](#)]
24. Pryor, S.C.; Nielsen, M.; Barthelmie, R.J.; Mann, J. Can Satellite Sampling of Offshore Wind Speeds Realistically Represent Wind Speed Distributions? Part II: Quantifying Uncertainties Associated with Distribution Fitting Methods. *J. Appl. Meteorol.* **2004**, *43*, 739–750. [[CrossRef](#)]
25. Cook, N.J. The Deaves and Harris ABL model applied to heterogeneous terrain. *J. Wind Eng. Ind. Aerodyn.* **1997**, *66*, 197–214. [[CrossRef](#)]

**Disclaimer/Publisher’s Note:** The statements, opinions and data contained in all publications are solely those of the individual author(s) and contributor(s) and not of MDPI and/or the editor(s). MDPI and/or the editor(s) disclaim responsibility for any injury to people or property resulting from any ideas, methods, instructions or products referred to in the content.